PLOS ONE

RESEARCH ARTICLE

Retinal astrocytes transcriptome reveals Cyp1b1 regulates the expression of genes involved in cell adhesion and migration

Juliana Falero-Perez[1], Christine M. Sorenson[2,3], Nader Sheibani[1,2,3,4,5]*

1 Department of Ophthalmology and Visual Sciences, University of Wisconsin School of Medicine and Public Health, Madison, Wisconsin, United States of America, **2** McPherson Eye Research Institute, University of Wisconsin School of Medicine and Public Health, Madison, Wisconsin, United States of America, **3** Department of Pediatrics, University of Wisconsin School of Medicine and Public Health, Madison, Wisconsin, United States of America, **4** Department of Biomedical Engineering, University of Wisconsin School of Medicine and Public Health, Madison, Wisconsin, United States of America, **5** Department of Cell and Regenerative Biology, University of Wisconsin School of Medicine and Public Health, Madison, Wisconsin, United States of America

* nsheibanikar@wisc.edu

Citation: Falero-Perez J, Sorenson CM, Sheibani N (2020) Retinal astrocytes transcriptome reveals Cyp1b1 regulates the expression of genes involved in cell adhesion and migration. PLoS ONE 15(4): e0231752. https://doi.org/10.1371/journal.pone.0231752

Editor: Daniel Bouvard, Institute for Advanced bioscience, FRANCE

Received: November 1, 2019

Accepted: April 1, 2020

Published: April 24, 2020

Data Availability Statement: All relevant data are within the paper.

Funding: The work in NS lab is supported by an unrestricted award from Research to Prevent Blindness to the Department of Ophthalmology and Visual Sciences, Retina Research Foundation, P30 EY016665, P30 CA014520, and R01 EY026078. CMS is supported by the RRF/Daniel M. Albert Chair. NS is a recipient of RPB Stein Innovation Award. JFP is supported by F31 EY027987 training grant. The funders had no role in study design,

Abstract

Astrocytes (AC) are the most abundant cells in the central nervous system. In the retina, astrocytes play important roles in the development and integrity of the retinal neurovasculature. Astrocytes dysfunction contributes to pathogenesis of a variety of neurovascular diseases including diabetic retinopathy. Recent studies have demonstrated the expression of Cyp1b1 in the neurovascular cells of the central nervous system including AC. We recently showed retinal AC constitutively express Cyp1b1, and global Cyp1b1-deficiency (*Cyp1b1*-/-) attenuates retinal ischemia-mediated neovascularization *in vivo* and the pro-angiogenic activity of retinal vascular cells *in vitro*. We also demonstrated that Cyp1b1 expression is a key regulator of retinal AC function. However, the underlying mechanisms involved need further investigation. Here we determined changes in the transcriptome profiles of *Cyp1b1*+/+ and *Cyp1b1*-/- retinal AC by RNA sequencing. We identified 585 differentially expressed genes, whose pathway enrichment analysis revealed the most significant pathways impacted in *Cyp1b1*-/- AC. These genes included those of axon guidance, extracellular matrix proteins and their receptors, cancer, cell adhesion molecules, TGF-β signaling, and the focal adhesion modulation. The expression of a selected set of differentially expressed genes was confirmed by RT-qPCR analysis. To our knowledge, this is the first report of RNAseq investigation of the retinal AC transcriptome and the molecular pathways impacted by Cyp1b1 expression. These results demonstrated an important role for Cyp1b1 expression in the regulation of various retinal AC functions, which are important in neurovascular development and integrity.

Introduction

The cytochrome P450 superfamily consists of many heme-containing monooxygenases. They are best known for their roles in drug metabolism. CYP1B1 is involved in many processes in the body, such as assisting with reactions that break down drugs and produce certain fats

data collection and analysis, decision to publish, or preparation of the manuscript.

Competing interests: The authors have declared that no competing interests exist.

(lipids). It is expressed in both adult and fetal human extrahepatic tissues, including most of the parenchymal and stromal tissues from brain, kidney, prostate, breast, cervix, uterus, ovary, lymph nodes [1], and ocular tissues [2, 3]. Mutations in this enzyme are a risk factor for the development of primary congenital glaucoma in humans [4]. However, the underlying cellular and molecular mechanisms are not fully revealed.

We previously showed expression of Cyp1b1 is essential for ischemia-mediated retinal neovascularization as occurs in retinopathy of prematurity, and the proangiogenic function of retinal vascular cells in culture [5–7]. However, how Cyp1b1 expression impacts these processes remained largely unknown. We showed Cyp1b1 is constitutively expressed in vascular endothelial cells and perivascular supporting cells from vascular beds of many organs including retina [5, 7]. Recently, we also demonstrated that Cyp1b1 is expressed in retinal astrocytes (AC), and *Cyp1b1*-/- retinal AC are more proliferative and migratory [8]. These cells produced increased amounts of fibronectin and its receptors αvβ3 and α5β1 integrins. However, production of inflammatory mediators such as BMP-7 and MCP-1 were decreased in *Cyp1b1*-/- AC. In addition, we observed a significant increase in CD38 expression when *Cyp1b1*-/- AC were challenged with H_2O_2 compared with *Cyp1b1*+/+ cells. *Cyp1b1*-/- AC also showed enhanced connexin 43 phosphorylation compared with *Cyp1b1*+/+ cells [8]. Thus, Cyp1b1-deficiency in AC was associated with increased resistance towards oxidative stress.

Astrocytes are the major cell type in the optic nerve head and are vital to the development and maintenance of the retinal astrocytic network and angiogenesis [9, 10]. Under pathological conditions, AC become reactive and contribute to various ocular pathologies including glaucoma and diabetic retinopathy [11]. However, there still much more to delineate regarding Cyp1b1 expression and function in AC. The few studies available to date have confirmed Cyp1b1 expression in AC and neurons, and its upregulation in a variety of gliomas [1, 12]. To our knowledge, we were first to report the impact of Cyp1b1 expression on retinal AC function. However, the intracellular pathways that mediate these activities of Cyp1b1 in AC remain elusive.

RNAseq is one transcriptomic approach where the total complement of RNAs from a given sample is isolated and sequenced using high-throughput technologies [13]. RNAseq technology has the potential to provide very useful, detailed information on the intracellular pathways impacted by Cyp1b1 expression, and identify the networks of genes involved. The purpose of the current study was to utilize this powerful technique to delineate the detailed molecular mechanisms of Cyp1b1 action in retinal AC by determining the changes in patterns of gene expression networks impacted by Cyp1b1 expression. The identification of genes whose expression is affected by the presence or absence of Cyp1b1 will provide additional clues to the intracellular mechanisms of Cyp1b1 action and function in retinal AC. This knowledge should lead to the discovery of new targets for modulation of Cyp1b1 activity and their potential therapeutic use.

Results

RNAseq analysis and global gene expression profiles of *Cyp1b1*+/+ and *Cyp1b1*-/- retinal AC

In order to investigate the impact of Cyp1b1 expression on the transcriptome profile of retinal AC, we performed RNAseq analysis of *Cyp1b1*+/+ and *Cyp1b1*-/- AC. All samples were uniquely barcoded, pooled and sequenced in one lane on an Illumina HiSeq 2500 platform. The average number of reads for *Cyp1b1*+/+ AC was $2.34x10^7$ and for *Cyp1b1*-/- AC was $2.32x10^7$. All sequence reads were mapped to the reference mouse genome using STAR (Spliced Transcripts Alignment to a Reference) [14]. To determine the expression level of various genes, mapped paired-end reads for genes were counted in each sample using RSEM (RNASeq by

Expectation Maximization) [15]. Gene expression was normalized by the method of trimmed mean of M-values (TMM), where the product of this factor and the library sizes defines the effective library size [16]. For each sample contrast, simple boxplots per sample expression distributions were constructed before and after TMM normalization (Fig 1A). Overall TMM values were similar in each sample, indicated by the uniform distributions.

Analysis of differentially expressed genes was performed with a glm using the edgeR package [17]. In order to decide which genes are differentially expressed (DEG), the adjusted p-value-not the raw p-value- was defined to be 0.05. To control the false discovery rate (FDR), a Benjamini-Hochberg correction was applied [18]. Fig 1B represents a Volcano plot showing DEG as red and blue dots denoting up- and down-regulated expression, respectively, at an adjusted p-value (FDR) significance threshold of 0.05. The gray dots reflect those genes with no evidence of statistically significant changes in expression. The

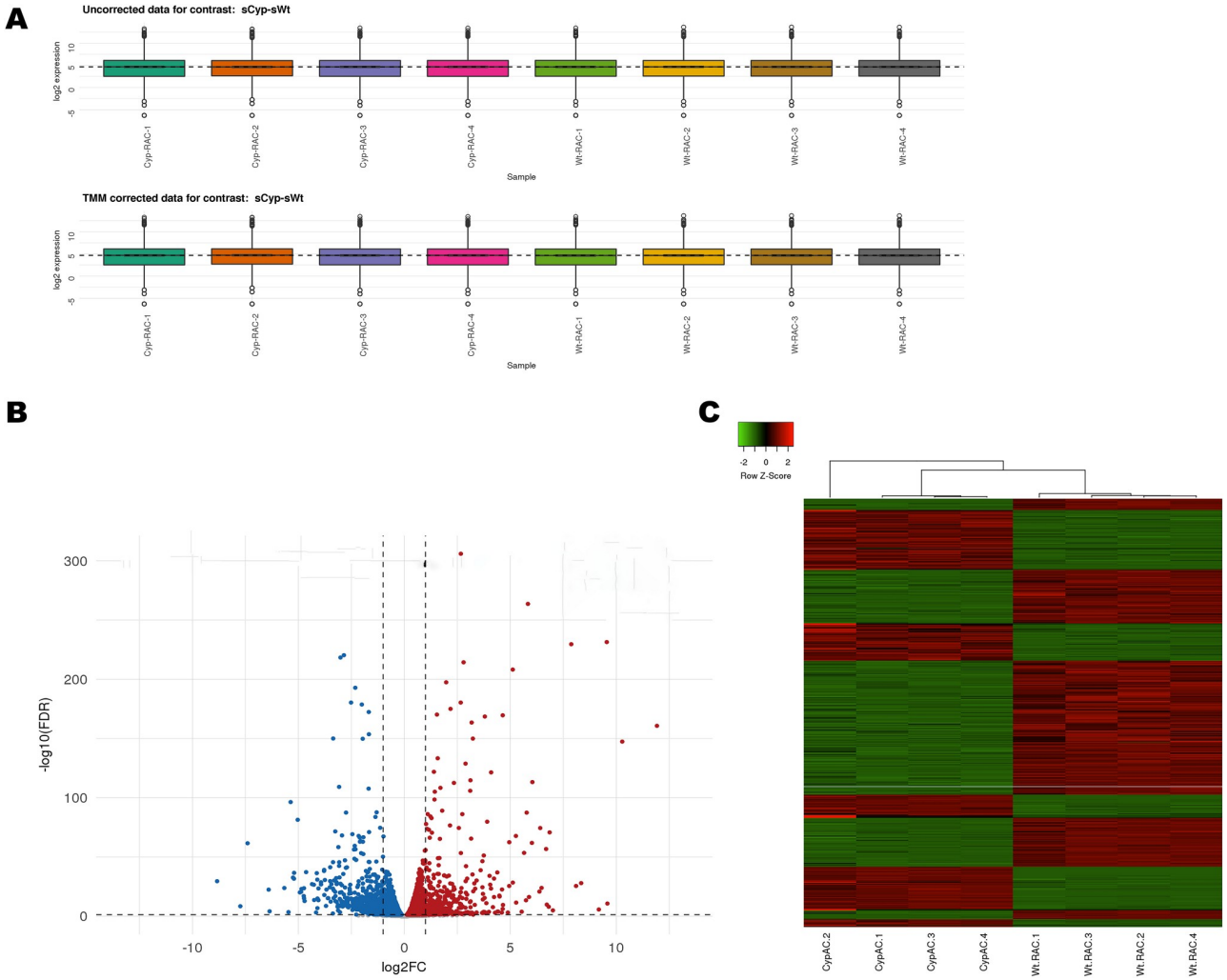

Fig 1. Gene expression profiles of the *Cyp1b1*+/+ and *Cyp1b1*-/- retinal AC. (A) Box plot showing overall TMM expression values for the *Cyp1b1*-/- AC and control samples. (B) Volcano plot showing differentially express genes. For each plot, the X-axis represents $\log_2$ FC and the Y-axis represents $-\log_{10}$ (FDR). The differentially expressed genes (DEG) are shown as red indicating increased expression and blue indicating decreased expression. (C) Hierarchical clustering of DEG. Red indicates increased expression and green indicates decreased expression. The DEG were defined as having absolute FC> 1.5 and an FDR< 0.05.

https://doi.org/10.1371/journal.pone.0231752.g001

two solid gray lines denote the boundary of a two-fold change. We also conducted a hierarchical clustering analysis of DEG from all samples with Ward's method of Euclidean distances [19], and created a heatmap with the heatmap function from Heatmapper: web-enabled heat mapping for all [20]. The results indicated that gene expression was similar in each group (Fig 1C).

The samples from the *Cyp1b1*+/+ and *Cyp1b1*-/- AC groups were assayed for DEG. The threshold was adjusted to Log2 fold-change with an absolute value of 2.0 and a p-value <1e-7. This yielded 585 transcripts (236 up- and 349-downregulated) for the downstream pathway analysis. The 20 most up- and downregulated genes are listed in Table 1. Within the top upregulated genes, we identified the following genes: Dsp (6.81-fold), Uty (11.92-fold), Cysltr1 (8.34-fold), Cdx2 (6.47-fold) and Kdm5d (10.28-fold). These genes have important roles in different biological and molecular processes including actin-mediated cell contraction, cardiac muscle contraction, oxidoreductase activity, and demethylase activity among others [21–24]. The top downregulated genes including Ptprf (-1.01-fold), Fgf10 (-1.03-fold), Prl2c3 (-1.034), Tgfb3 (-1.04-fold), Mical1 (-1.05-fold), Ndrg2 (-1.05-fold), Ptgs1 (-1.0487-fold), Aplp1 (-1.08-fold), and Steap3 (-1.08-fold) have important roles in processes including cell proliferation, apoptosis, regulation of DNA replication, and metabolic processes among others [25–27]. DEG (585 total) were subjected to Gene Ontology to establish a connection with the biological processes and molecular functions that these genes contribute to (Fig 2).

Pathway enrichment analysis, conducted using KEGG (Kyoto Encyclopedia of Genes and Genomes) [28–30] as a mapping database, 57 pathways were identified with significance level of 0.05. To cut down on the list the $P < 0.002$ was applied. The pathways with multiple points of commonality and overlap among the Axon guidance, extracellular matrix-receptor interactions, pathways in cancer, cell adhesion molecules, TGF-β signaling pathways, and the focal adhesion were identified as most significantly enriched pathways (Table 2).

To validate the RNAseq findings, RT-qPCR were performed on newly extracted RNA from *Cyp1b1*+/+AC and *Cyp1b1*-/-AC. From each KEGG pathway, we selected key genes with important roles in angiogenesis, apoptosis, cell proliferation, cell migration, metabolism and inflammation. We selected 27 genes (Cxcl12, Cxcl11, Col1a2, Arnt2, Fgf7, Mmp2, Bmp7, Thsb2, Bmp8b, Cdh3, Cdh4, Gdf5, Cd80, Cldn1, Lefty1, Cysltr1, Drd4, Aldh1a7, Cbr2, B3gnt3, Cbr3, Ldhb, Gatm, Adcy7, Cacna1d, Ccl7, and Mapk13) involved in the pathways identified in Table 2. We examined changes in their expression by RT-qPCR (Figs 3 and 4). The results obtained with RT-qPCR showed similar changes in expression as those obtained from the RNAseq studies (Table 3). However, the changes in the expression of a number of these genes did not reach significant levels. These included Cxcl12, Cysltr1, Cacna1d, Col1a2, Aldh1a7, Cbr2, B3gnt3, Gatm, and Lefty1.

Discussion

In this study we used RNAseq analysis to determine the global transcriptome profile of *Cyp1b1* +/+ and *Cyp1b1*-/- AC from mouse retina. We identified 585 DEG, whose pathway analysis revealed the most significant biological functions. These included the Axon guidance, extracellular matrix (ECM)-receptor interactions, pathways in cancer, cell adhesion molecules, TGF-β signaling, and the focal adhesion regulation. We also found that some of the top downregulated genes were involved in biological and molecular processes including actin-mediated cell contraction, cardiac muscle contraction, cell proliferation, apoptosis and metabolic processes.

Our findings here were consistent with the results of our previous studies showing increased proliferation and migration of *Cyp1b1*-/- AC. Activation of AC proliferation and

Table 1. Top 20 up- and down-regulated genes in Cyp1b1-/-AC.

Symbol	Description	Log2FC	p-value	FDR
Up-regulated				
Eif2s3y	eukaryotic translation initiation factor 2, subunit 3, structural gene Y-linked	12.01499	0	0
Uty	ubiquitously transcribed tetratricopeptide repeat gene, Y chromosome	11.91885	3.6E-164	1.9E-161
Ddx3y	DEAD (Asp-Glu-Ala-Asp) box polypeptide 3, Y-linked	11.79096	0	0
Kdm5d	lysine (K)-specific demethylase 5D	10.28087	8.9E-151	4E-148
Gm43302	predicted gene 43302	9.580986	1.21E-12	2E-11
Rpl15-ps2	ribosomal protein L15, pseudogene 2	9.550535	2.2E-235	3.8E-232
Bmp8b	bone morphogenetic protein 8b	8.847732	0	0
Cysltr1	cysteinyl leukotriene receptor 1	8.342675	1.93E-30	1.16E-28
Gm26760	predicted gene, 26760	8.102196	5.58E-28	2.97E-26
Gm10020	predicted pseudogene 10020	7.874941	1.6E-233	2.5E-230
Gm6969	predicted pseudogene 6969	6.85453	7.82E-74	1.63E-71
Dsp	desmoplakin	6.813457	9.78E-10	1.13E-08
Actg-ps1	actin, gamma, pseudogene 1	6.722348	1.08E-11	1.58E-10
Sgsm1	small G protein signaling modulator 1	6.689262	1.12E-59	1.78E-57
Cdx2	caudal type homeobox 2	6.474141	2.61E-26	1.27E-24
Gm38312	predicted gene, 38312	6.410902	1.62E-77	3.66E-75
Oxct2b	3-oxoacid CoA transferase 2B	6.374568	4.13E-23	1.59E-21
AI593442	expressed sequence AI593442	6.040882	1.6E-116	6E-114
Gm45315	predicted gene 45315	6.018783	7.76E-65	1.3E-62
Adarb2	adenosine deaminase, RNA-specific, B2	5.88212	2.23E-18	6.17E-17
Down-regulated				
Ptprf	protein tyrosine phosphatase, receptor type, F	-1.009044	3.978E-53	5.686E-51
Gprc5a	G protein-coupled receptor, family C, group 5, member A	-1.02267	2.718E-12	4.306E-11
Vax2	ventral anterior homeobox 2	-1.025959	5.515E-10	6.507E-09
Fgf10	fibroblast growth factor 10	-1.028563	3.695E-21	1.264E-19
Stard9	START domain containing 9	-1.030828	2.45E-13	4.349E-12
Lmo1	LIM domain only 1	-1.031322	5.887E-17	1.438E-15
Prl2c3	prolactin family 2, subfamily c, member 3	-1.034173	1.076E-22	4.025E-21
Gm27177	predicted gene 27177	-1.034225	3.073E-17	7.67E-16
Tgfb3	transforming growth factor, beta 3	-1.035388	2.308E-12	3.687E-11
Flrt3	fibronectin leucine rich transmembrane protein 3	-1.038403	8.71E-09	8.981E-08
Acsf2	acyl-CoA synthetase family member 2	-1.040813	9.692E-12	1.426E-10
Ppic	peptidylprolyl isomerase C	-1.042228	5.977E-32	3.847E-30
Eif3j1	eukaryotic translation initiation factor 3, subunit J1	-1.042647	4.709E-42	5.158E-40
Mical1	microtubule associated monooxygenase, calponin and LIM domain containing 1	-1.046611	1.687E-09	1.899E-08
Ndrg2	N-myc downstream regulated gene 2	-1.047743	2.791E-13	4.941E-12
Ptgs1	prostaglandin-endoperoxide synthase 1	-1.0487	5.856E-29	3.273E-27
Cbr3	carbonyl reductase 3	-1.050294	2.114E-16	4.933E-15
Slfn8	schlafen 8	-1.061261	4.262E-23	1.64E-21
Aplp1	amyloid beta (A4) precursor-like protein 1	-1.075804	8.932E-14	1.662E-12
Steap3	STEAP family member 3	-1.08044	5.467E-14	1.046E-12

The cutoff criteria for this list was any DEG with a FC> 5.88 for upregulation and FC> -1.009 for downregulation.

https://doi.org/10.1371/journal.pone.0231752.t001

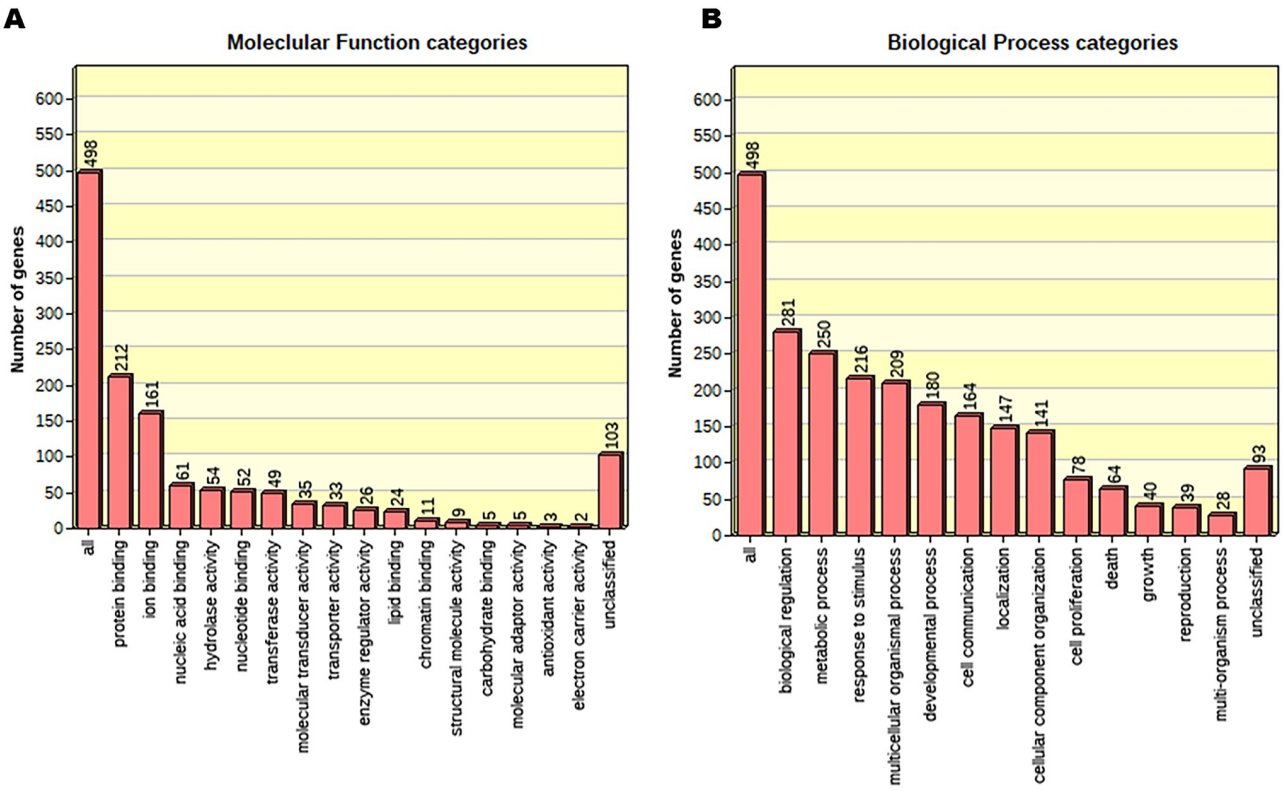

Fig 2. The biological process and molecular functions significantly impacted in *Cyp1b1*-/- AC. (A) Bar graph of the biological process categories. (B) Bar graph of the molecular function. DEG were subjected to GO enrichment analysis having absolute FC> 2 and a FDR< 0.05.

https://doi.org/10.1371/journal.pone.0231752.g002

migration is important in repair of injuries in the central nervous system (CNS) and scar formation [31, 32]. AC migration is regulated by various factors, among which transforming growth factor-β (TGF-β) plays an important role [33]. In AC, TGF-β suppresses cell proliferation by inducing $p15^{INK4B}$ expression in a Smad3-dependent manner [34]. This is consistent with our findings that showed the downregulation of TGF-β in *Cyp1b1*-/- AC. The upregulation of Smad genes in *Cyp1b1* -/- AC was associated with the enhanced pathways in axon guidance and cell proliferation.

Our results showed changes in Cxcl12, (also known as SDF-1). Cxcl12 is one of the most studied chemokines that induce cell proliferation and migration by binding to its receptor. Under normal conditions, Cxcl12 expression in the CNS is relatively low. However, its expression is upregulated when the CNS is affected by trauma, ischemia, inflammation or infection [35]. Enhanced Cxcl12 expression promotes proliferation of radial glia like cells after traumatic brain injury in rats [36]. Others have shown its therapeutic value by promoting autophagy and migration via PI3K-AKT-mTOR pathway [37].

We recently showed that Cyp1b1 deficiency affects retinal AC ECM production and expression of integrin receptors [8]. We also showed upregulation of cadherins, laminin, and tenascin. These molecules are well known for their roles in cell adhesion [38], and were associated with changes in adhesion observed in *Cyp1b1*-/- retinal AC [8]. Cadherin-4 (also known as R-cadherin) is involved in retinal angiogenesis during development. Dorrell et al. [39] used antibodies or peptides to neutralize R-cadherin, which prevented the normal formation of the retinal vascular network in newborn mice. They also showed that R-cadherin plays a crucial role

Table 2. Pathway enrichment analysis of significantly changed genes.

KEGG Pathway name	Pathway Rank	GENES	FDR adjusted enrichment score p-value
Axon guidance	1	Sema3c, Unc5d, Sema5a, Sema3g, Ngef, Lrrc4c, Sema6b, Cxcl12, Unc5c, Sema4f, Plxnb1, Sema6a	3.32e-07
ECM-receptor interaction	2	Itga1, Col1a2, Lama2, Tnxb, Spp1, Lama5, Col5a3, Npnt, Thbs2	4.79e-06
Pathways in cancer	3	Dapk1, Arnt2, Wnt5b, Lama2, Pgf, Hhip, Apc2, Fgf7, Pax8, Lama5, Wnt4, Tgfb3, Ar, Mmp2, Fgf10	1.31e-05
Cell adhesion molecules (CAMs)	4	Vcan, Cdh4, Cd80, Cldn1, Vcam1, Cd34, Ptprf, Cdh3, Icam1	0.0002
TGF-beta signaling pathway	5	Tgfb3, Gdf5, Fst, Lefty1, Bmp7, Bmp8b, Thbs2	0.0002
Focal adhesion	6	Itga1, Col1a2,Lama2,Pgf, Tnxb, Spp1, Lama5, Col5a3, Myl12b,Thbs2	0.0002
Neuroactive ligand-receptor interaction	7	Lepr, Adra1d, Htr1b, Gria4, Grid2, Htr2a, Cysltr1,Drd4, Calcrl, Grid1	0.0020
Metabolic pathways	8	Mgat3, Itpkb, Cda, Xylb, Pla2g4b, Abat, Ckb, Ass1, Isyna1, Aldh1a7, Aldh1a1, Nnmt, Cbr2, B3gnt3, Cbr3, Gldc, Eno2, Ptgs1, Bdh2, Ldhb, Gatm, St3gal1, Sardh	0.0041
Calcium signaling pathway	9	Adcy7, Cacna1d, Itpkb, Cacna1h, Adra1d, Htr2a, Cysltr1	0.0058
Cytokine-cytokine receptor interaction	10	Lepr, Ccl7, Bmp7, Tgfb3, Tnfsf10, Cxcl11, Cxcl12, Gdf5	0.0077
MAPK signaling pathway	11	Mapk13, Tgfb3, Cacna1d, Cacna1h, Pla2g4b, Fgf10, Fgf7	0.0277

Significantly changed transcriptome. Column 1 lists the canonical KEGG pathway name, column 2 lists the pathway enrichment score rank in terms of p-value determined by hypergeometric test, column 3 lists the genes that mapped to the KEGG pathway, and column 4 shows the FDR adjusted p-value of significance of the pathway enrichment score.

https://doi.org/10.1371/journal.pone.0231752.t002

in the endothelial–astrocyte interactions [39, 40]. Thus, Cyp1b1 expression may impact AC interactions with EC.

Oxidative stress is implicated in many neurodegenerative diseases. Cytochrome P450 activities are generally involved in ROS production due to their involvement in the metabolism of steroids, fat-soluble vitamins, fatty acids, eicosanoids, drugs, carcinogens, and other xenobiotic chemicals [41–43]. CYP enzymes can generate superoxide and hydrogen peroxide through uncoupling reactions, for more details see [44]. We have demonstrated an important role for Cyp1b1 as a modulator of cellular redox state [45]. Studies utilizing vascular cells derived from *Cyp1b1*-/- mice showed an increase in oxidative stress in vascular endothelial cells and perivascular supporting cells [5, 7, 46]. In contrast, *Cyp1b1*-/- retinal AC did not show an increase in oxidative stress compared to *Cyp1b1*+/+ cells under basal conditions [8]. This is consistent with minimal changes in expression of genes that affect cellular redox state in the absence of Cyp1b1. However, incubation of these cells with known inducers of oxidative stress could reveal changes in genes that modulate oxidative stress. This notion is supported by our studies demonstrating that *Cyp1b1*-/- AC elicit a significantly more robust response in expression of CD38 when challenged with H_2O_2 compared with *Cyp1b1*+/+ cells [47]. Thus, the elucidation of the mechanisms behind AC resilience to oxidative stress, especially in the absence of Cyp1b1, needs further investigation.

Cytochrome P450 enzymes are involved in metabolism of drugs, and are major source of variability in drug pharmacokinetics and responses. However, in some cases they can also activate compounds consumed in food, converting pro-carcinogens to carcinogens [48]. CYP proteins, involved in steroid or retinoic acid metabolism, could promote or suppress tumors development through hormonal control [49, 50]. Genetic variability could play a role if a polymorphism affected a CYP protein involved in such processes [51]. Our study found multiple genes in the cancer pathway that are associates with the progression or suppression of cancer

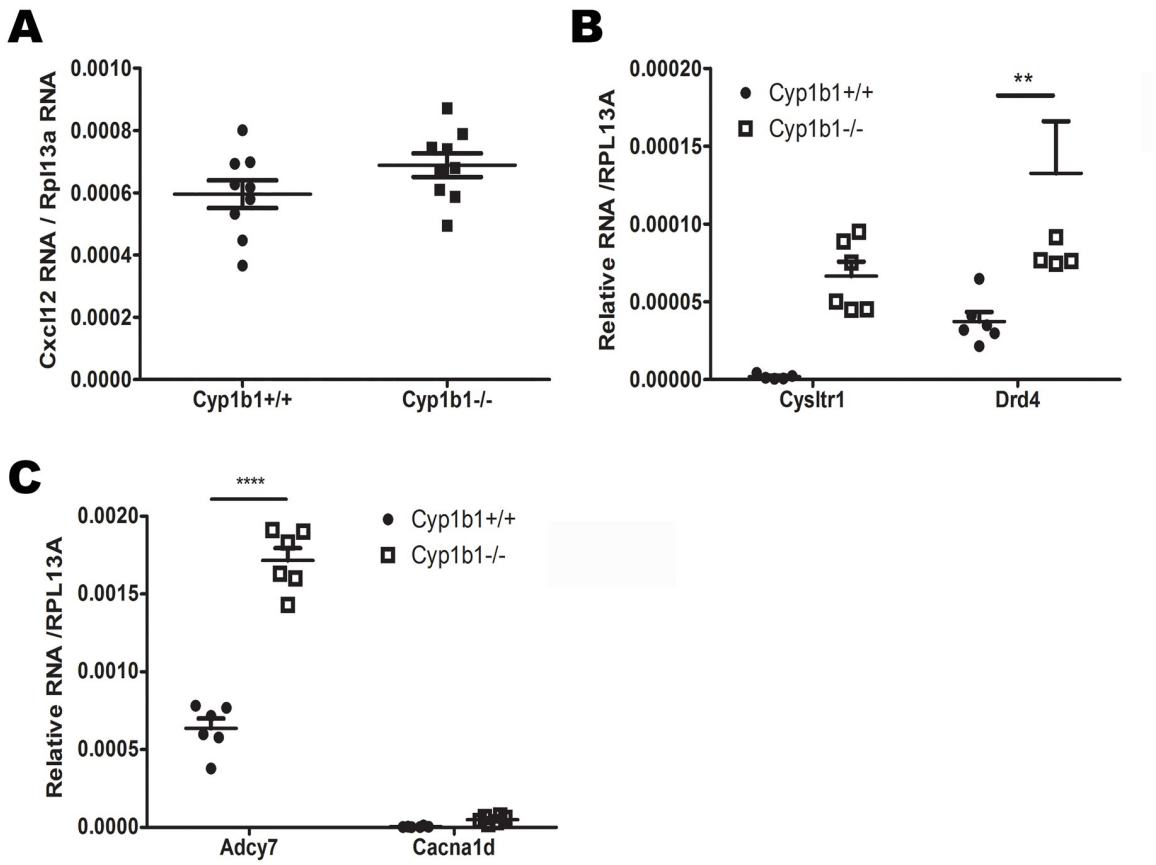

Fig 3. RT-qPCR validation of DEG from different pathways. (A) Genes related to the axon guidance pathway. (B) Genes related to the Neuroactive ligand-receptor interaction pathway. (C) Genes related to the Calcium signaling pathway. (**P<0.01, ****P<0.0001, n≥ 6).

https://doi.org/10.1371/journal.pone.0231752.g003

such as laminin, Tgfβ3, Hhip, Arnt2 and Mmp2 [52–54]. Mmp2 was upregulated in this pathway and is implicated in cancer cell migration [55]. A previous study using a microarray analysis, demonstrated that the increased expression of Mmp2 is involved in invasiveness of malignant glioma [56, 57], an observation that is consistent with our findings. Thus, Cyp1b1 expression has an important role in modulating AC migration by suppressing Mmp2 expression.

A limitation of our studies is the use of cells prepared from mix genders. Our initial in vivo and in vitro vascular cell culture studies did not demonstrate a gender bias in the noted phenotypes with *Cyp1b1*-deficiency. However, our gene expression studies here showed some of the differentially expressed genes in Cyp1b1 null cells are sex linked: Uty; Y-chromosome, Cysltr1; X-chromosome, and Kdm5d; Y-chromosome. Thus, Cyp1b1-deficiency impact on gene expression, and likely noted phenotypes, could be deferentially impacted by gender. Future studies will further address the gender contributions to various phenotypes noted with *Cyp1b1*-deficiecny.

In summary, RNAseq technology was used to investigate the transcriptome profiles of retinal AC and how Cyp1b1 expression modulates their cellular functions. A pathway analysis of DEG indicated the most significantly enriched pathways included Axon guidance, ECM-receptor interactions, as well as cancer and other pathways (cell proliferation, focal adhesion, and cell adhesion). Our transcriptomic approach in this investigation, which relied on

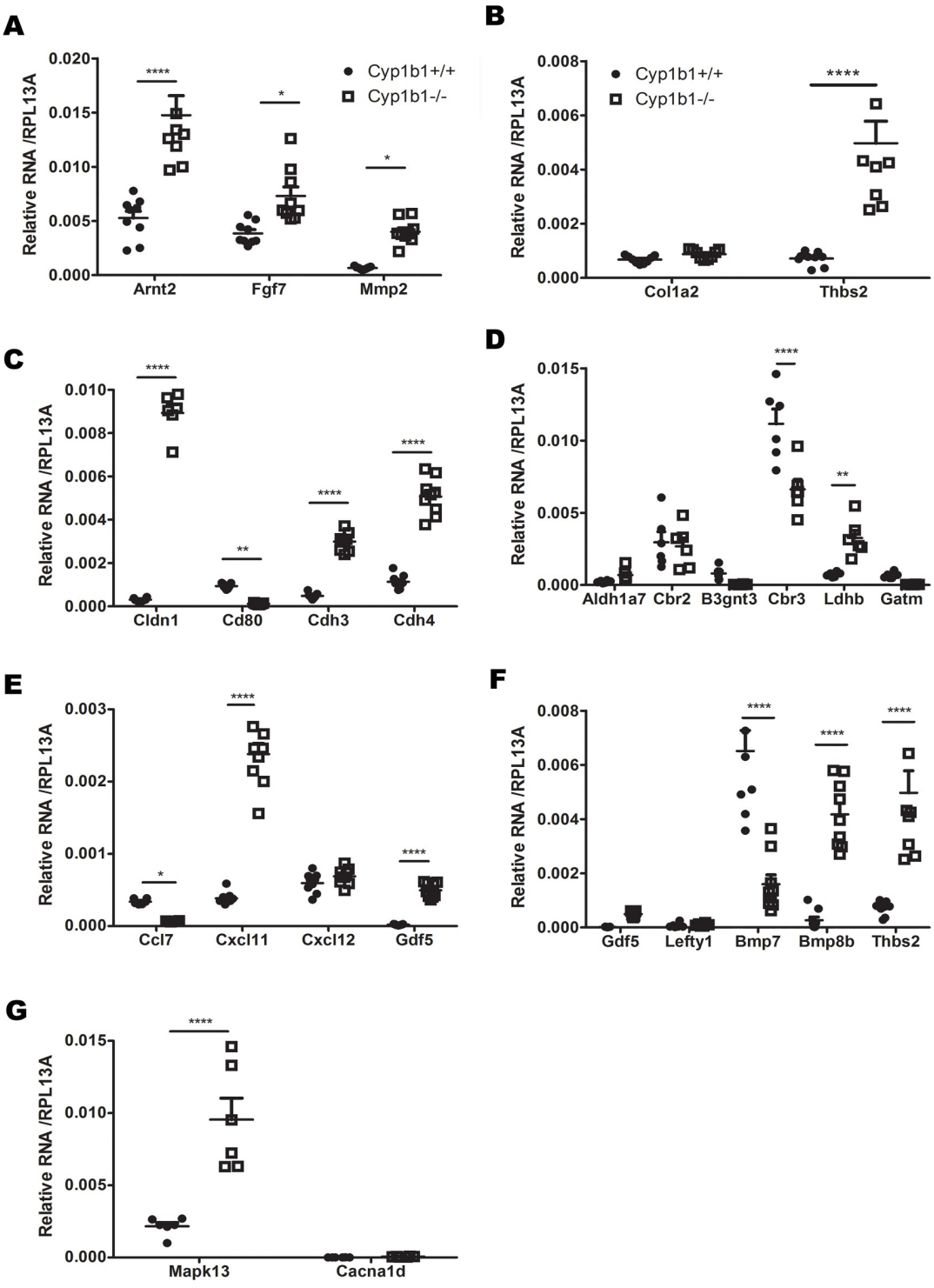

Fig 4. RT-qPCR validation of DEG from different pathways. (A) Genes related to the Cancer pathway. (B) Genes related to the ECM-Receptor and Focal adhesion pathways. (C) Genes related to the Cell adhesion molecules pathways. (D) Genes related to the metabolic pathways. (E) Genes related to the Cytokine-Cytokine interaction pathways. (F) Genes related to the TGF-β signaling pathway. (G) Genes related to the MAPK signaling pathways. ($^{*}P<0.05$, $^{**}P<0.01$, $^{****}P<0.0001$, $n \geq 6$).

https://doi.org/10.1371/journal.pone.0231752.g004

Table 3. Differentially expressed gene selected for RT-qPCR validation.

KEGG pathway name	Symbol	Gene Description	Log_2FC	p-value
Axon Guidance	Cxcl12	chemokine (C-X-C motif) ligand 12	1.10	2.39E-89
ECM-receptor interaction	Col1a2	collagen, type I, alpha 2	5.74	1.69E-15
	Thbs2	thrombospondin 2	2.67	4.62E-12
Pathways in cancer	Arnt2	aryl hydrocarbon receptor nuclear translocator 2	1.70	1.28E-111
	Fgf7	fibroblast growth factor 7	1.28	6.02E-86
	Mmp2	matrix metallopeptidase 2	5.28	1.77E-13
Cell adhesion molecules	Cdh4	cadherin 4 (retinal)	3.23	2.45E-153
	Cd80	CD80 antigen	-3.52	7.99E-27
	Cldn1	claudin 1	4.64	4.05E-173
	Cdh3	cadherin 3 (placental)	3.75	3.80E-54
TGF-β signaling	Gdf5	growth differentiation factor 5	4.65	2.08E-11
	Lefty1	left right determination factor 1	2.62	1.32E-12
	Bmp7	bone morphogenetic protein 7	-2.31	2.04E-59
	Bmp8b	bone morphogenetic protein 8b	8.85	0
	Thbs2	thrombospondin 2	2.67	4.62E-12
Focal adhesion	Col1a2	collagen, type I, alpha 2	5.74	1.69E-15
	Thbs2	thrombospondin 2	2.67	4.62E-12
Neuroactive ligand- receptor interaction	Cysltr1	cysteinyl leukotriene receptor 1	8.34	1.93E-30
	Drd4	dopamine receptor D4	3.32	1.86E-11
Metabolic pathways	Aldh1a7	aldehyde dehydrogenase family 1, subfamily A7	3.34	1.25E-25
	Cbr2	carbonyl reductase 2	2.20	3.12E-10
	B3gnt3	UDP-GlcNAc:betaGal beta-1,3-N-acetylglucosaminyltransferase 3	-5.21	
	Cbr3	carbonyl reductase 3	-1.05	2.114E-16
	Ldhb	lactate dehydrogenase B	2.15	7.57E-21
	Gatm	glycine amidinotransferase (L-arginine:glycine amidinotransferase)	-4.63	6.11E-40
Calcium signaling	Adcy7	adenylate cyclase 7	1.34	2.44E-15
	Cacna1d	calcium channel, voltage-dependent, L type, alpha 1D subunit	3.87	5.65E-13
	Cysltr1	cysteinyl leukotriene receptor 1	8.34	1.93E-30
Cytokine-cytokine receptor interaction	Ccl7	chemokine (C-C motif) ligand 7	-2.40	9.08E-10
	Bmp7	bone morphogenetic protein 7	-2.31	2.04E-59
	Cxcl11	chemokine (C-X-C motif) ligand 11	2.96	2.05E-20
	Cxcl12	chemokine (C-X-C motif) ligand 12	1.10	2.39E-89
	Gdf5	growth differentiation factor 5	4.65	2.08E-11
MAPK signaling	Mapk13 (P38-delta)	mitogen-activated protein kinase 13	1.66	5.24E-52
	Cacna1d	calcium channel, voltage-dependent, L type, alpha 1D subunit	3.87	5.65E-13
	Fgf7	fibroblast growth factor 7	1.28	6.02E-86

The expression of selected genes related to the KEGG pathways were validated by RT-qPCR. LogFC and p-values were obtained from RNAseq analysis.

https://doi.org/10.1371/journal.pone.0231752.t003

RNAseq, was powerful and effective way to allow us to obtain a global view of genes whose expression are impacted by Cyp1b1, likely in a gender dependent manner.

Materials and methods

Ethics statement

All animal experiments were performed in accordance to the Association for Research in Vision and Ophthalmology Statement for the Use of Animals in Ophthalmic and Vision

Research and were approved by the Institutional Animal Care and Use Committee of the University of Wisconsin School of Medicine and Public Health (the assurance number A3368-01). Animals were sacrificed according to an approved protocol by CO2 asphyxiation.

Isolation and culture of Cyp1b1-/- retinal AC

Retinal AC were isolated from mouse retina by collecting retinas from one litter of 4-week-old (6 to 7- mix gender) mice using a dissecting microscope, as previously described by us with greater than 98% purity [8, 58]. Briefly, retinas (12 to 14) were rinsed with serum-free Dulbecco's Modified Eagle's Medium (DMEM), pooled in a 60 mm dish, minced and digested for 45 min with collagenase Type I (1 mg/ml; Worthington, Lakewood, NJ) in serum-free DMEM at 37˚C. Cells were rinsed in DMEM containing 10% fetal bovine serum (FBS) and centrifuged for 5 min at 400 xg. Digested cells were rinsed again in DMEM containing 10% FBS and filtered through a double layer of sterile 40 μm nylon mesh (Sefar America Inc., Fisher Scientific, Hanover Park, IL). Cells were centrifuged for 5 min at 400 xg and medium was aspirated. Cells were washed twice with DMEM containing 10% FBS, resuspended in 1 ml of DMEM containing 10% FBS in a 1.5 ml microfuge tube and incubated with rat-anti-mouse CD31 (Mec13.3; BD Biosciences) coated with sheep anti-rat magnetic beads, and were gently rocked for 1 h at 4˚C. Using a Dynal magnetic tube holder, cells not bound to magnetic beads were collected and washed in DMEM containing 10% FBS. Cells were plated in growth medium in a single well of a 24 well plate coated with human fibronectin (2 μg/ml in serum-free DMEM; BD Biosciences, Bedford, MA), and incubated at 33˚C with 5% CO2. The cells bound to magnetic beads are generally used to remove retinal EC as we described [58]. Retinal AC were grown in DMEM containing 10% FBS, 2 mM L-glutamine, 2 mM sodium pyruvate, 20 mM HEPES, 1% nonessential amino acids, 100 μg/ml streptomycin, 100 U/ml penicillin, freshly added heparin at 55 U/ml (Sigma, St. Louis, MO), endothelial growth supplement 100 μg/ml (Sigma), and the murine recombinant interferon-γ (R&D, Minneapolis, MN) at 44 U/ml. Cells were maintained at 33˚C with 5% CO2. Cells were progressively passed to larger plates, maintained, and propagated in 1% gelatin-coated 60 mm dishes. For all experiments, cells were used at 70–80% confluence unless stated otherwise.

RNA purification

Total RNA from Cyp1b1+/+ and Cyp1b1-/- retinal AC was purified using RNeasy Mini kit according to manufacturer's protocol with the DNAse treatment step to eliminate traces of genomic DNA (Qiagen, Germantown, MD). The quality and quantity of the total RNA were measured using an Agilent Model 2100 Bioanalyzer, and samples showing a RIN >8 were selected for further analysis. Samples were stored in RNase-free water and kept at -80˚C until further processing.

RNA sequencing

Eight samples of purified RNA (4 from *Cyp1b1*+/+ retinal AC and 4 from *Cyp1b1* -/- retinal AC) were subsequently subjected to a double round of poly-A mRNA purification, fragmented, and primed for cDNA library synthesis using the TruSeq RNA sample preparation kit (RS-122-9004). All procedures were carried out according to the manufacturer's instructions (Illumina, San Diego, CA). Following validation (Agilent 2100 Bioanalyzer, DNA 1000) and normalization, samples were clustered (TruSeq pairedend cluster kit v3-cBot-HS, PE-401-3001) followed by paired-end sequencing (100 bp; TruSeq SBS kit v3-HS 200 cycles, FC-401-3001) on a HiSeq2500. The following quality control statistics were used to evaluate the technical quality of the experiments; (1) combined per cycle base quality, (2) per cycle base

frequencies, (3) per cycle average base quality, (4) relative 3k-mer diversity, (5) Phred quality distribution, (6) mean quality distribution, (7) read length distribution and (8) read occurrence distribution using the trimming software skewer [59]. Low-abundance genes with a read count below a threshold of 1.0 in two or more samples were excluded. To compare gene expression between Cyp1b1+/+AC and Cyp1b1-/-AC, samples were normalized by trimmed mean of M-values (TMM) using Edge R (version 2.5 of Bioconductor) software [16]. After the inspection of preliminary data, transcript reads were aligned to the preassembled selected reference genome sequence using STAR (Spliced Transcripts Alignment to a Reference) using the default settings [14]. Transcript abundance were performed by using RSEM (RNASeq by Expectation Maximization) [15]. Subsequently, differential analysis of significant changes in gene expression was performed with a glm using the edgeR package [17] in the different genotype pairs (e.g. *Cyp1b1*+/+ vs. *Cyp1b1* -/-). All sequence data have been deposited in the Gene Expression Omnibus with accession number GSE145103.

Quantitative RT-PCR

Total RNA from retinal AC was extracted using mirVana PARIS kit (Invitrogen). The cDNA synthesis was performed from 1 μg of total RNA using Sprint RT Complete-Double PrePrimed kit (Clontech, Mountain View, CA). One μl of each cDNA (dilution 1∶10) was used as template in qPCR assays, performed in triplicate of three biological replicates on Mastercycler Realplex (Eppendorf) using the SYBR-Green qPCR Premix (Clontech). Amplification parameters were as follows: 95˚C for 2 min; 40 cycles of amplification (95˚C for 15 sec, 60˚C for 40 sec); dissociation curve step (95˚C for 15 sec, 60˚C for 15 sec, 95˚C for 15 sec). Standard curves were generated from known quantities for each of the target gene of linearized plasmid DNA. Ten times dilution series were used for each known target, which were amplified using SYBR-Green qPCR. The linear regression line for ng of DNA was determined from relative fluorescent units (RFU) at a threshold fluorescence value (Ct) to quantify gene targets from cell extracts by comparing the RFU at the Ct to the standard curve, normalized by the simultaneous amplification of RpL13a, a housekeeping gene. All primer sequence used are listed in Table 4.

Biological interaction network and KEGG pathway enrichment analysis

Pathway Enrichment Analysis was performed with WEBGESTALT web analysis software (http://bioinfo.vanderbilt.edu/wg2/) by mapping significantly changed genes to corresponding KEGG enrichment pathways, Gene Ontology enrichment and conducting a hypergeometric statistical test with significant level <0.05 after multiple testing correction [60–62]. Significance for pathway level enrichment was defined as having an enrichment score False Discovery Rate (FDR) corrected p-value < 0.05.

Statistical analysis

RNA-seq data were analyzed and gene expressions were normalized by the method of trimmed mean of M-values (TMM) and glm using the edgeR package, respectively. This yielded a total of 13,575 genes. KEGG pathway enrichment analysis cut-off criteria of FDR<0.05 with a $|FC|>2$ was apply. RT-PCR data were analyzed with student's unpaired t-test (2-tailed) or one-way ANOVA with post-Bonferroni's test for multiple comparisons. $P\leq 0.05$ was considered significant. Data are presented as Mean ± SEM from cells with $n\geq 6$ (as indicated in figure legends). All data analysis was done in GraphPad Prism or Microsoft Excel.

Table 4. Primers to validate differentially express genes.

Gene	Amplicon size (bp)	primer	Primer Sequence (5'->3')	Length	Gene accession
Cxcl12	116	F	ctgtgcccttcagattgttg	20	NM_001012477.2
		R	ctctgcgccccttgttta	18	
Cxcl11	93	F	tgctgagatgaacaggaaggt	21	NM_019494.1
		R	cgcccctgtttgaacataag	20	
Col1a2	69	F	ctggtgcacagggtgtga	18	NM_007743.3
		R	ctcctgcttgacctggagtt	20	
Arnt2	104	F	tgcacttcggaaaactccat	20	NM_007488.3
		R	cgagagcccatacacatgc	19	
Fgf7	78	F	ttactccatagttctgcaaccagt	24	NM_008008.4
		R	tgttgcccttcccttcataa	20	
Mmp2	75	F	gggcttctgtcctgacca	18	NM_008610.3
		R	aagttcttggtgtaggtgtagatcg	25	
Bmp8b	70	F	ctgtatgaactccaccaaccac	22	NM_028189.3
		R	ggggatgatatctggcttca	20	
Cdh3	75	F	aggcccagctaacacatgac	20	NM_001037809.5
		R	acaaggccacggtgtctc	18	
Cdh4	60	F	ttcctggctgctgacaatg	19	NM_009867.3
		R	gtagatctgcagggtcccagt	21	
Gdf5	73	F	tttattgacaaagggcaagatg	22	NM_008109.3
		R	aggcactgatgtcaaacacg	20	
Cd80	127	F	ttcgtctttcacaagtgtcttca	23	NM_009855.2
		R	tgccagtagattcggtcttca	21	
Cldn1	92	F	actccttgctgaatctgaacagt	23	NM_016674.4
		R	ggacacaaagattgcgatcag	21	
Lefty1	92	F	actcagtatgtggccctgcta	21	NM_010094.4
		R	aacctgcctgccacctct	18	
Cysltr1	95	F	aaggtgctgaggtaccagatagag	24	NM_021476.5
		R	aatcacagcccttgagaagc	20	
Drd4	137	F	cccaccaactacttcatcgtg	21	NM_007878
		R	gccatgagcgtgtcacag	18	
Aldh1a7	85	F	gtttgcagatgccgacttg	19	NM_011921.2
		R	cgctgcaacacaaatctgac	20	
Cbr2	109	F	gcccatgtcacctttcctaa	20	NM_007621.2
		R	ttacccggatcttgtgtgg	19	
B3gnt3	115	F	gcaaatacaaccgactgctg	20	NM_028189.3
		R	cactccaggaaaaggacctg	20	
Cbr3	60	F	aacgttagcgggagagatga	20	NM_173047.3
		R	cccttgatgtgggaaagaatc	21	
Ldhb	86	F	gtagtgggcgttggacaagt	20	NM_001316322.1
		R	acatccaccagggcaagtt	19	
Gatm	103	F	ggtgcactacatcggctctc	20	NM_025961.5
		R	acaggaatttcgggaggaa	19	
Cacna1d	60	F	gaagctgcttgaccaagttgt	21	NM_001302637.1
		R	aacttccccacggttacctc	20	
Ccl7	91	F	ttctgtgcctgctgctcata	20	NM_013654.3
		R	ttgacatagcagcatgtggat	21	
MAPK13	63	F	caggctggccttgagtctt	19	NM_011950.2

(*Continued*)

Table 4. (Continued)

Gene	Amplicon size (bp)	primer	Primer Sequence (5'->3')	Length	Gene accession
		R	ccagggctacacagtaagatcc	22	
Adcy7		F	gagccttccagacgtccat	19	NM_007406.2
	70	R	aggaggataacggcattgg	19	

https://doi.org/10.1371/journal.pone.0231752.t004

Acknowledgments

The authors thank the University of Wisconsin- Madison Biotechnology Center Gene Expression Center & DNA Sequencing Facility for providing library preparation and next generation sequencing services. We thank Sammed Mandape for assistance with the bioinformatics analysis.

Author Contributions

Conceptualization: Juliana Falero-Perez, Christine M. Sorenson, Nader Sheibani.

Data curation: Juliana Falero-Perez.

Formal analysis: Juliana Falero-Perez, Christine M. Sorenson, Nader Sheibani.

Funding acquisition: Nader Sheibani.

Investigation: Juliana Falero-Perez, Christine M. Sorenson, Nader Sheibani.

Methodology: Juliana Falero-Perez.

Supervision: Christine M. Sorenson, Nader Sheibani.

Writing – original draft: Juliana Falero-Perez, Christine M. Sorenson, Nader Sheibani.

Writing – review & editing: Juliana Falero-Perez, Christine M. Sorenson, Nader Sheibani.

References

1. Muskhelishvili L, Thompson PA, Kusewitt DF, Wang C, Kadlubar FF. In situ hybridization and immunohistochemical analysis of cytochrome P450 1B1 expression in human normal tissues. The journal of histochemistry and cytochemistry: official journal of the Histochemistry Society. 2001; 49:229–36. https://doi.org/10.1177/002215540104900210 PMID: 11156691.
2. Stoilov I, Akarsu AN, Sarfarazi M. Identification of three different truncating mutations in cytochrome P4501B1 (CYP1B1) as the principal cause of primary congenital glaucoma (Buphthalmos) in families linked to the GLC3A locus on chromosome 2p21. Hum Mol Genet. 1997; 6(4):641–7. https://doi.org/10.1093/hmg/6.4.641 PMID: 9097971.
3. Stoilov I, Akarsu AN, Alozie I, Child A, Barsoum-Homsy M, Turacli ME, et al. Sequence analysis and homology modeling suggest that primary congenital glaucoma on 2p21 results from mutations disrupting either the hinge region or the conserved core structures of cytochrome P4501B1. Am J Hum Genet. 1998; 62(3):573–84. https://doi.org/10.1086/301764 PMID: 9497261
4. Zhao Y, Sorenson CM, Sheibani N. Cytochrome P450 1B1 and Primary Congenital Glaucoma. J Ophthalmic Vis Res. 2015; 10(1):60–7. Epub 2015/05/26. https://doi.org/10.4103/2008-322X.156116 PMID: 26005555.
5. Tang Y, Scheef EA, Wang S, Sorenson CM, Marcus CB, Jefcoate CR, et al. CYP1B1 expression promotes the proangiogenic phenotype of endothelium through decreased intracellular oxidative stress and thrombospondin-2 expression. Blood. 2009; 113(3):744–54. Epub 2008/11/14. https://doi.org/10.1182/blood-2008-03-145219 PMID: 19005183
6. Tang Y, Scheef EA, Gurel Z, Sorenson CM, Jefcoate CR, Sheibani N. CYP1B1 and endothelial nitric oxide synthase combine to sustain proangiogenic functions of endothelial cells under hyperoxic stress. Am J Physiol Cell Physiol. 2010; 298(3):C665–78. Epub 2009/12/25. https://doi.org/10.1152/ajpcell.00153.2009 PMID: 20032512.

7. Palenski TL, Sorenson CM, Jefcoate CR, Sheibani N. Lack of Cyp1b1 promotes the proliferative and migratory phenotype of perivascular supporting cells. Lab Invest. 2013; 93(6):646–62. Epub 2013/04/10. https://doi.org/10.1038/labinvest.2013.55 PMID: 23568032

8. Falero-Perez J, Sorenson CM, Sheibani N. Cyp1b1-deficient retinal astrocytes are more proliferative and migratory and are protected from oxidative stress and inflammation. Am J Physiol Cell Physiol. 2019; 316(6):C767–c81. Epub 2019/03/21. https://doi.org/10.1152/ajpcell.00021.2019 PMID: 30892936.

9. Fruttiger M. Development of the retinal vasculature. Angiogenesis. 2007; 10(2):77–88. https://doi.org/10.1007/s10456-007-9065-1 PMID: 17322966.

10. Stone J, Makarov F, Hollander H. The glial ensheathment of the soma and axon hillock of retinal ganglion cells. Vis Neurosci. 1995; 12(2):273–9. Epub 1995/03/01. https://doi.org/10.1017/s0952523800007951 PMID: 7786848

11. Fruttiger M, Calver AR, Kruger WH, Mudhar HS, Michalovich D, Takakura N, et al. PDGF mediates a neuron-astrocyte interaction in the developing retina. Neuron. 1996; 17(6):1117–31. https://doi.org/10.1016/s0896-6273(00)80244-5 PMID: 8982160

12. Barnett JA, Urbauer DL, Murray GI, Fuller GN, Heimberger AB. Cytochrome P450 1B1 expression in glial cell tumors: an immunotherapeutic target. Clin Cancer Res. 2007; 13(12):3559–67. Epub 2007/06/19. https://doi.org/10.1158/1078-0432.CCR-06-2430 PMID: 17575219

13. Wang Z, Gerstein M, Snyder M. RNA-Seq: a revolutionary tool for transcriptomics. Nat Rev Genet. 2009; 10(1):57–63. Epub 2008/11/19. https://doi.org/10.1038/nrg2484 PMID: 19015660

14. Dobin A, Davis CA, Schlesinger F, Drenkow J, Zaleski C, Jha S, et al. STAR: ultrafast universal RNA-seq aligner. Bioinformatics. 2013; 29(1):15–21. Epub 2012/10/30. https://doi.org/10.1093/bioinformatics/bts635 PMID: 23104886

15. Li B, Dewey CN. RSEM: accurate transcript quantification from RNA-Seq data with or without a reference genome. BMC Bioinformatics. 2011; 12:323. Epub 2011/08/06. https://doi.org/10.1186/1471-2105-12-323 PMID: 21816040

16. Robinson MD, Oshlack A. A scaling normalization method for differential expression analysis of RNA-seq data. Genome Biol. 2010; 11(3):R25. Epub 2010/03/04. https://doi.org/10.1186/gb-2010-11-3-r25 PMID: 20196867

17. Robinson MD, McCarthy DJ, Smyth GK. edgeR: a Bioconductor package for differential expression analysis of digital gene expression data. Bioinformatics. 2010; 26(1):139–40. Epub 2009/11/17. https://doi.org/10.1093/bioinformatics/btp616 PMID: 19910308

18. Reiner A, Yekutieli D, Benjamini Y. Identifying differentially expressed genes using false discovery rate controlling procedures. Bioinformatics. 2003; 19(3):368–75. Epub 2003/02/14. https://doi.org/10.1093/bioinformatics/btf877 PMID: 12584122

19. Ward JH. Hierarchical Grouping to Optimize an Objective Function. Journal of the American Statistical Association. 1963; 58(301):236–44. https://doi.org/10.1080/01621459.1963.10500845

20. Babicki S, Arndt D, Marcu A, Liang Y, Grant JR, Maciejewski A, et al. Heatmapper: web-enabled heat mapping for all. Nucleic Acids Res. 2016; 44(W1):W147–53. Epub 2016/05/18. https://doi.org/10.1093/nar/gkw419 PMID: 27190236

21. Rungger-Brandle E, Achtstatter T, Franke WW. An epithelium-type cytoskeleton in a glial cell: astrocytes of amphibian optic nerves contain cytokeratin filaments and are connected by desmosomes. J Cell Biol. 1989; 109(2):705–16. Epub 1989/08/01. https://doi.org/10.1083/jcb.109.2.705 PMID: 2474553

22. Piromkraipak P, Sangpairoj K, Tirakotai W, Chaithirayanon K, Unchern S, Supavilai P, et al. Cysteinyl Leukotriene Receptor Antagonists Inhibit Migration, Invasion, and Expression of MMP-2/9 in Human Glioblastoma. Cell Mol Neurobiol. 2018; 38(2):559–73. Epub 2017/06/11. https://doi.org/10.1007/s10571-017-0507-z PMID: 28600709

23. Zhao T, Gan Q, Stokes A, Lassiter RN, Wang Y, Chan J, et al. beta-catenin regulates Pax3 and Cdx2 for caudal neural tube closure and elongation. Development. 2014; 141(1):148–57. Epub 2013/11/29. https://doi.org/10.1242/dev.101550 PMID: 24284205

24. Atala A. Re: Resistance to Docetaxel in Prostate Cancer is Associated with Androgen Receptor Activation and Loss of KDM5D Expression. J Urol. 2017; 197(1):154–5. Epub 2016/12/17. https://doi.org/10.1016/j.juro.2016.10.010 PMID: 27979512

25. Zhang Y, Alexander PB, Wang XF. TGF-beta Family Signaling in the Control of Cell Proliferation and Survival. Cold Spring Harb Perspect Biol. 2017; 9(4). Epub 2016/12/07. https://doi.org/10.1101/cshperspect.a022145 PMID: 27920038

26. Tian X, Yang C, Yang L, Sun Q, Liu N. PTPRF as a novel tumor suppressor through deactivation of ERK1/2 signaling in gastric adenocarcinoma. OncoTargets and therapy. 2018; 11:7795–803. Epub 2018/11/23. https://doi.org/10.2147/OTT.S178152 PMID: 30464527

27. Deng W, Wang Y, Zhao S, Zhang Y, Chen Y, Zhao X, et al. MICAL1 facilitates breast cancer cell proliferation via ROS-sensitive ERK/cyclin D pathway. J Cell Mol Med. 2018; 22(6):3108–18. Epub 2018/03/11. https://doi.org/10.1111/jcmm.13588 PMID: 29524295

28. Aoki-Kinoshita KF, Kanehisa M. Gene annotation and pathway mapping in KEGG. Methods Mol Biol. 2007; 396:71–91. Epub 2007/11/21. https://doi.org/10.1007/978-1-59745-515-2_6 PMID: 18025687

29. Kanehisa M. The KEGG database. Novartis Found Symp. 2002; 247:91–101; discussion -3, 19–28, 244–52. Epub 2003/01/24. PMID: 12539951

30. Ogata H, Goto S, Sato K, Fujibuchi W, Bono H, Kanehisa M. KEGG: Kyoto Encyclopedia of Genes and Genomes. Nucleic Acids Res. 1999; 27(1):29–34. Epub 1998/12/10. https://doi.org/10.1093/nar/27.1.29 PMID: 9847135

31. Fawcett JW, Asher RA. The glial scar and central nervous system repair. Brain Res Bull. 1999; 49 (6):377–91. Epub 1999/09/14. https://doi.org/10.1016/s0361-9230(99)00072-6 PMID: 10483914.

32. Saadoun S, Papadopoulos MC, Watanabe H, Yan D, Manley GT, Verkman AS. Involvement of aquaporin-4 in astroglial cell migration and glial scar formation. J Cell Sci. 2005; 118(Pt 24):5691–8. Epub 2005/11/24. https://doi.org/10.1242/jcs.02680 PMID: 16303850

33. Huang XQ, Zhang XY, Wang XR, Yu SY, Fang SH, Lu YB, et al. Transforming growth factor beta1-induced astrocyte migration is mediated in part by activating 5-lipoxygenase and cysteinyl leukotriene receptor 1. Journal of neuroinflammation. 2012; 9:145. Epub 2012/06/28. https://doi.org/10.1186/1742-2094-9-145 PMID: 22734808

34. Rich JN, Zhang M, Datto MB, Bigner DD, Wang XF. Transforming growth factor-beta-mediated p15 (INK4B) induction and growth inhibition in astrocytes is SMAD3-dependent and a pathway prominently altered in human glioma cell lines. J Biol Chem. 1999; 274(49):35053–8. Epub 1999/11/27. https://doi.org/10.1074/jbc.274.49.35053 PMID: 10574984

35. Trettel F, Di Castro MA, Limatola C. Chemokines: Key Molecules that Orchestrate Communication among Neurons, Microglia and Astrocytes to Preserve Brain Function. Neuroscience. 2019. Epub 2019/08/04. https://doi.org/10.1016/j.neuroscience.2019.07.035 PMID: 31376422

36. Mao W, Yi X, Qin J, Tian M, Jin G. CXCL12 promotes proliferation of radial glia like cells after traumatic brain injury in rats. Cytokine. 2019; 125:154771. Epub 2019/08/11. https://doi.org/10.1016/j.cyto.2019.154771 PMID: 31400639

37. Gao D, Tang T, Zhu J, Tang Y, Sun H, Li S. CXCL12 has therapeutic value in facial nerve injury and promotes Schwann cells autophagy and migration via PI3K-AKT-mTOR signal pathway. Int J Biol Macromol. 2019; 124:460–8. Epub 2018/11/06. https://doi.org/10.1016/j.ijbiomac.2018.10.212 PMID: 30391592

38. Hillen AEJ, Burbach JPH, Hol EM. Cell adhesion and matricellular support by astrocytes of the tripartite synapse. Prog Neurobiol. 2018; 165–167:66–86. Epub 2018/02/15. https://doi.org/10.1016/j.pneurobio.2018.02.002 PMID: 29444459

39. Dorrell MI, Aguilar E, Friedlander M. Retinal vascular development is mediated by endothelial filopodia, a preexisting astrocytic template and specific R-cadherin adhesion. Invest Ophthalmol Vis Sci. 2002; 43 (11):3500–10. PMID: 12407162.

40. Shan WS, Tanaka H, Phillips GR, Arndt K, Yoshida M, Colman DR, et al. Functional cis-heterodimers of N- and R-cadherins. J Cell Biol. 2000; 148(3):579–90. Epub 2000/02/09. https://doi.org/10.1083/jcb.148.3.579 PMID: 10662782

41. Hrycay EG, Bandiera SM. Involvement of Cytochrome P450 in Reactive Oxygen Species Formation and Cancer. Adv Pharmacol. 2015; 74:35–84. Epub 2015/08/04. https://doi.org/10.1016/bs.apha.2015.03.003 PMID: 26233903

42. Hassan HM, Guo H, Yousef BA, Guerram M, Hamdi AM, Zhang L, et al. Role of Inflammatory and Oxidative Stress, Cytochrome P450 2E1, and Bile Acid Disturbance in Rat Liver Injury Induced by Isoniazid and Lipopolysaccharide Cotreatment. Antimicrob Agents Chemother. 2016; 60(9):5285–93. Epub 2016/06/22. https://doi.org/10.1128/AAC.00854-16 PMID: 27324775

43. Lu D, Ma Y, Zhang W, Bao D, Dong W, Lian H, et al. Knockdown of cytochrome P450 2E1 inhibits oxidative stress and apoptosis in the cTnT(R141W) dilated cardiomyopathy transgenic mice. Hypertension. 2012; 60(1):81–9. Epub 2012/06/06. https://doi.org/10.1161/HYPERTENSIONAHA.112.191478 PMID: 22665122

44. Veith A, Moorthy B. ROLE OF CYTOCHROME P450S IN THE GENERATION AND METABOLISM OF REACTIVE OXYGEN SPECIES. Current opinion in toxicology. 2018; 7:44–51. Epub 2018/03/13. https://doi.org/10.1016/j.cotox.2017.10.003 PMID: 29527583

45. Falero-Perez J, Song YS, Sorenson CM, Sheibani N. CYP1B1: A key regulator of redox homeostasis. Trends in cell & molecular biology. 2018; 13:27–45. Epub 2018/01/01.

46. Zhao Y, Wang S, Sorenson CM, Teixeira L, Dubielzig RR, Peters DM, et al. Cyp1b1 mediates periostin regulation of trabecular meshwork development by suppression of oxidative stress. Mol Cell Biol. 2013;

33(21):4225–40. Epub 08/28. https://doi.org/10.1128/MCB.00856-13 Epub 2013 Aug 26. PMID: 23979599.

47. Ma Y, Wu D, Ding X, Ying W. CD38 plays key roles in both antioxidation and cell survival of H2O2-treated primary rodent astrocytes. International journal of physiology, pathophysiology and pharmacology. 2014; 6(2):102–8. Epub 2014/07/25. PMID: 25057336

48. Mittal B, Tulsyan S, Kumar S, Mittal RD, Agarwal G. Cytochrome P450 in Cancer Susceptibility and Treatment. Adv Clin Chem. 2015; 71:77–139. Epub 2015/09/29. https://doi.org/10.1016/bs.acc.2015.06.003 PMID: 26411412

49. Gajjar K, Martin-Hirsch PL, Martin FL. CYP1B1 and hormone-induced cancer. Cancer Lett. 2012; 324:13–30. https://doi.org/10.1016/j.canlet.2012.04.021 PMID: 22561558.

50. Bolton JL, Thatcher GR. Potential mechanisms of estrogen quinone carcinogenesis. Chem Res Toxicol. 2008; 21(1):93–101. Epub 2007/12/07. https://doi.org/10.1021/tx700191p PMID: 18052105

51. Zanger UM, Schwab M. Cytochrome P450 enzymes in drug metabolism: regulation of gene expression, enzyme activities, and impact of genetic variation. Pharmacol Ther. 2013; 138(1):103–41. https://doi.org/10.1016/j.pharmthera.2012.12.007 PMID: 23333322.

52. Givant-Horwitz V, Davidson B, Reich R. Laminin-induced signaling in tumor cells. Cancer Lett. 2005; 223(1):1–10. Epub 2005/05/14. https://doi.org/10.1016/j.canlet.2004.08.030 PMID: 15890231

53. Xu J, Lamouille S, Derynck R. TGF-beta-induced epithelial to mesenchymal transition. Cell Res. 2009; 19(2):156–72. Epub 2009/01/21. https://doi.org/10.1038/cr.2009.5 PMID: 19153598

54. Sun H, Ni SJ, Ye M, Weng W, Zhang Q, Zhang M, et al. Hedgehog Interacting Protein 1 is a Prognostic Marker and Suppresses Cell Metastasis in Gastric Cancer. Journal of Cancer. 2018; 9(24):4642–9. Epub 2018/12/28. https://doi.org/10.7150/jca.27686 PMID: 30588248

55. Xu X, Wang Y, Chen Z, Sternlicht MD, Hidalgo M, Steffensen B. Matrix metalloproteinase-2 contributes to cancer cell migration on collagen. Cancer Res. 2005; 65(1):130–6. Epub 2005/01/25. PMID: 15665288

56. Hur JH, Park MJ, Park IC, Yi DH, Rhee CH, Hong SI, et al. Matrix metalloproteinases in human gliomas: activation of matrix metalloproteinase-2 (MMP-2) may be correlated with membrane-type-1 matrix metalloproteinase (MT1-MMP) expression. J Korean Med Sci. 2000; 15(3):309–14. Epub 2000/07/15. https://doi.org/10.3346/jkms.2000.15.3.309 PMID: 10895974

57. Ramachandran RK, Sorensen MD, Aaberg-Jessen C, Hermansen SK, Kristensen BW. Expression and prognostic impact of matrix metalloproteinase-2 (MMP-2) in astrocytomas. PLoS One. 2017; 12(2): e0172234. Epub 2017/02/25. https://doi.org/10.1371/journal.pone.0172234 PMID: 28234925

58. Scheef E, Wang S, Sorenson CM, Sheibani N. Isolation and characterization of murine retinal astrocytes. Mol Vis. 2005; 11:613–24. PMID: 16148882.

59. Jiang H, Lei R, Ding SW, Zhu S. Skewer: a fast and accurate adapter trimmer for next-generation sequencing paired-end reads. BMC Bioinformatics. 2014; 15:182. Epub 2014/06/14. https://doi.org/10.1186/1471-2105-15-182 PMID: 24925680

60. Kirov S, Ji R, Wang J, Zhang B. Functional annotation of differentially regulated gene set using WebGestalt: a gene set predictive of response to ipilimumab in tumor biopsies. Methods Mol Biol. 2014; 1101:31–42. Epub 2013/11/16. https://doi.org/10.1007/978-1-62703-721-1_3 PMID: 24233776

61. Zhang B, Kirov S, Snoddy J. WebGestalt: an integrated system for exploring gene sets in various biological contexts. Nucleic Acids Res. 2005; 33(Web Server issue):W741–8. Epub 2005/06/28. https://doi.org/10.1093/nar/gki475 PMID: 15980575

62. Wang J, Duncan D, Shi Z, Zhang B. WEB-based GEne SeT AnaLysis Toolkit (WebGestalt): update 2013. Nucleic Acids Res. 2013; 41(Web Server issue):W77–83. Epub 2013/05/25. https://doi.org/10.1093/nar/gkt439 PMID: 23703215